Received: 23 May 2022 | Revised: 31 October 2022 | Accepted: 23 November 2022

DOI: 10.1002/hbm.26167

RESEARCH ARTICLE

WILEY

Fetal behavior during MRI changes with age and relates to network dynamics

Lanxin Ji[1] | Amyn Majbri[1] | Cassandra L. Hendrix[1] | Moriah E. Thomason[1,2,3]

[1]Department of Child & Adolescent Psychiatry, New York University School of Medicine, New York, New York, USA

[2]Department of Population Health, New York University School of Medicine, New York, New York, USA

[3]Neuroscience Institute, New York University School of Medicine, New York, New York, USA

Correspondence
Lanxin Ji, Department of Child & Adolescent Psychiatry, New York University School of Medicine, 1 Park Ave, 8th Floor, New York, NY 10016, USA.
Email: lanxin.ji@nyulangone.org

Funding information
National Institutes of Health, Grant/Award Numbers: DA050287, ES032294, MH110793, MH122447

Abstract

Fetal motor behavior is an important clinical indicator of healthy development. However, our understanding of associations between fetal behavior and fetal brain development is limited. To fill this gap, this study introduced an approach to automatically and objectively classify long durations of fetal movement from a continuous four-dimensional functional magnetic resonance imaging (fMRI) data set, and paired behavior features with brain activity indicated by the fMRI time series. Twelve-minute fMRI scans were conducted in 120 normal fetuses. Postnatal motor function was evaluated at 7 and 36 months age. Fetal motor behavior was quantified by calculating the frame-wise displacement (FD) of fetal brains extracted by a deep-learning model along the whole time series. Analyzing only low motion data, we characterized the recurring coactivation patterns (CAPs) of the supplementary motor area (SMA). Results showed reduced motor activity with advancing gestational age (GA), likely due in part to loss of space ($r = -.51$, $p < .001$). Evaluation of individual variation in motor movement revealed a negative association between movement and the occurrence of coactivations within the left parietotemporal network, controlling for age and sex ($p = .003$). Further, we found that the occurrence of coactivations between the SMA to posterior brain regions, including visual cortex, was prospectively associated with postnatal motor function at 7 months ($r = .43$, $p = .03$). This is the first study to pair fetal movement and fMRI, highlighting potential for comparisons of fetal behavior and neural network development to enhance our understanding of fetal brain organization.

KEYWORDS
coactivation patterns, deep learning, fetal fMRI, fetal motor behavior, motor cortex, motor development, network dynamics

1 | INTRODUCTION

Complexity of fetal motor behavior increases as the nervous system matures across gestation. Studies of individual variation show that more active fetuses tend to have higher behavioral and neurological maturation as neonates (DiPietro et al., 2010) and infants (Richards & Newbery, 1938). Studies have also documented that fetal motor behavior can predict postnatal mental development (Hayat et al., 2018), and even childhood temperament (Dipietro et al., 2018). Apart from reflecting neurobehavioral maturation in typical development, fetal behavior also informs risk of postnatal congenital disorders (De Vries & Fong, 2007; Hayat & Rutherford, 2018) and poor perinatal

outcomes (De Vries & Fong, 2007). For instance, decreased fetal movement has been associated with preterm birth, elevated rates of cesarean delivery (Dutton et al., 2012), mild language delay (Hayat et al., 2018), and neonatal stroke (Hielkema & Hadders-Algra, 2016). Although fetal motor behavior is an important marker of development, methods for quantifying fetal movement are rather limited, which has constrained our ability to study these at a large scale.

Traditionally, Ultrasound Sonography and state-of-art Cine Magnetic Resonance Imaging (MRI) have been used to visualize and assess fetal motor behavior (Hayat & Rutherford, 2018). Fetal motor behavior is most frequently characterized in terms of "general movements" and "isolated movements," where general movements are characterized by a global sequence of movement of variable speed, amplitude, direction, and fluency (Guzzetta et al., 2003; Prechtl & Einspieler, 1997), and isolated movements involve distinctive sequencing of particular body parts (Fagard et al., 2018). Utilization of these techniques has led to important insight into the progression of motor maturation that occurs across human gestation.

A new application with potential to advance understanding of fetal motor maturation is application of deep-learning techniques to automatically and objectively classify long durations of fetal movement data from continuous four-dimensional data sets. Recently, a Convolutional Neural Network (CNN) trained by 1241 manually traced fetal brain functional MRI (fMRI) images, achieved rapid and accurate automated brain masking for all volumes across the time series (Rutherford et al., 2021). This advancement in technology enables the objective and automatic quantification of fetal movement—a feat that was previously difficult to achieve. Although fetal brain fMRI typically only provides information about head motion, rather than whole body movements, it nonetheless presents an interesting use case, as the Blood Oxygen Level Dependent (BOLD) time-series data carry crucial information about brain activity that can be paired with volume of activity over the scan. Opportunity to examine associations between fetal motor behavior and fetal brain development can be easy to overlook because motion of the fetus is typically regarded as a contaminant in fMRI imaging data that unconditionally interferes with reliable measurement (Thomason, 2020). However, it is standard in fetal fMRI studies to acquire more data than is needed and to discard high-motion volumes (van den Heuvel et al., 2018). Thus, it is possible to pair neural connectomes or network analyses from low movement data with objective quantification of fetal activity across the full scan to begin to understand associations between fetal behavior and fetal brain development.

An aspect of neural connectomes that has recently gained attention is examining network reorganization over the scan. So-called "dynamic" functional connectivity (DFC) takes into account natural oscillations in the strength of connections between pairs or sets of regions. Rather than regarding neural connectivity as a "static" representation of connection strength, this technique remains sensitive to alterations in and out of primary patterns of organization that may be reflective of brain states or natural shifts in connectivity that may underlie mental experiences. Among the existing set of DFC methods, one focusing on recurring coactivation patterns (CAPs) of the brain by regarding individual fMRI volumes as basic units of analysis, has been shown a valid and robust method to capture clear but distinct brain states (Liu et al., 2013; Liu et al., 2018). Despite remarkable progress in understanding the human fetal connectome in health and disease, there are no studies that have analyzed the dynamic nature of fetal neural functional connectivity, which is critical for our understanding of human brain maturation.

The objectives of this study were to utilize CAPs to assess time-varying neural network dynamics in fetal brain data, to introduce a novel fMRI-based approach for assessing fetal behavior, and to test hypotheses about developmental change and associations between motor activity and brain development. Specifically, we expect that the observed movement of the fetus will relate to neural dynamics expressed in regions connected to the motor cortex. We also expect fetal motion to decline with advancing gestational age (GA; e.g., due to reduced space) and that behavior and neural dynamics in utero have potential to predict postnatal motor outcomes.

2 | MATERIALS AND METHODS

2.1 | Participants

Healthy mothers were recruited during routine obstetrical appointments at Hutzel Women's Hospital in Detroit, MI, between 2011 and 2018. Inclusionary criteria included maternal age ≥ 18 years old, native English speaking, singleton pregnancy, and normal fetal brain anatomy as assessed by ultrasound and MRI examination. All study procedures were approved by the Wayne State University Human Investigation Committee.

MRI visits occurred when fetuses were between 22- and 39-week GA. For quality control, fetuses were excluded if they were scanned before 25-week GA ($n = 9$) or had low birthweight or were born very preterm (<1800 g or <33 weeks GA; $n = 14$). Subjects younger than 25 GA were excluded based on prior evidence that intrinsic network connectivity emerges at approximately the 25th GA (Jakab et al., 2014). We also excluded fetuses with few low-motion functional volumes or excessive head motion within low-motion data chunks (1.5 mm max excursion, 0.5 mm mean, rotational: >2° or <100 low-motion volumes; $n = 22$). The final sample consisted of 120 fetuses (see Table 1). After birth, 77 infants completed standardized assessments of their motor development at 7 months of age and 89 infants completed the same assessment at 36 months of age.

2.2 | fMRI acquisition and preprocessing

Fetal functional MRI images were collected, using a 3 T Siemens Verio 70 cm open-bore system with a 550 g abdominal 4-channel Siemens Flex coil (Siemens). For each participant, two runs of 6 min-fMRI scan (180 volumes per run) or one run of 12-min scan (360 volumes per run) were collected with the following gradient echo planar imaging sequence: TR = 2000 ms; TE = 30 ms; flip-angle: 80°, slice-gap: none;

TABLE 1 Participant demographics

	Final sample included in fetal CAP analysis ($n = 120$)	Final sample included in fetal motor behavior assessment ($n = 98$)	Postnatal sample included at 7 months ($n = 77$)	Postnatal sample included at 36 months ($n = 89$)
	Mean (SD) or *N* (%)	Mean (SD) or *N* (%)	Mean (SD) or *N* (%)	Mean (SD) or *N* (%)
Demographics				
Maternal age at fetal MRI	25.35 (4.55) years	25.11 (4.28) years	26.22 (4.88) years	25.51 (5.12) years
Maternal GA at fetal MRI	32.95 (3.76) weeks	32.44 (3.90) weeks	33.19 (3.55) weeks	32.84 (3.75) weeks
Maternal race				
African American	98 (82%)	84 (86%)	60 (78%)	74 (83%)
Caucasian	10 (8%)	6 (6%)	7 (9%)	7 (8%)
Bi-racial	5 (4%)	2 (2%)	4 (6%)	3 (3%)
Asian American	1 (1%)	1 (1%)	1 (1%)	1 (1%)
Latina	1 (1%)	1 (1%)	0	0
Not disclosed	5 (4%)	4 (4%)	5 (6%)	4 (4%)
GA at birth	39.09 (1.45) weeks	39.04 (1.53) weeks	39.13(1.39) weeks	38.98 (1.61) weeks
Preterm (<36 weeks)	4 (3%)	4 (4%)	1 (1%)	4 (5%)
Birth weight	3236.70 (512.83) g	3245.73 (536.20) g	3238.34 (498.21) g	3169.89 (519.29) g
Fetal sex	53 (44%) females	47 (48%) females	33 (43%) females	43 (48%) females

voxel-size: 3.4 × 3.4 × 4 mm^3; matrix-size: 96 × 96 × 25 voxels. This sequence was repeated when time permitted. Longer TE is preferred for fetal EPI, as T2* relaxation times in fetal brains of the cortical tissue is about twice as high as those in adults (Blazejewska et al., 2017).

Preprocessing was performed using combined functions provided by FSL (https://fsl.fmrib.ox.ac.uk/fsl/fslwiki/) and Statistical Parametric Mapping (SPM12) software (http://icatb.source-forge.net). In brief, fMRI volumes with significant head motion were manually identified, using FSL image viewer, and excluded. Remaining segments of relatively low-motion fMRI data are henceforth referred to as "the low-motion segments." These are the data that were retained for further analyses. Next, Brainsuite (Shattuck & Leahy, 2002) was used to manually draw three-dimensional masks around single reference images, which were then applied to all other volumes for brain extraction within the same low-motion segment. For each 4D low-motion segment, manual masking, reorientation, motion correction, and normalization to a 32-week fetal brain template (Serag et al., 2012) were performed. Preprocessed segments were then concatenated to form a single series and realignment was applied to correct potential misalignment between segments. This was followed by individual-level denoising based on Independent Component Analysis (ICA) with "FSL Melodic," and spatial smoothing with a 4-mm FWHM Gaussian kernel. After concatenation of selected low-motion segments, number of retained volumes across subjects was mean = 165.00 (*SD* = 52.72). The average length of a single low-motion segment was 21.61 volumes (*SD* = 15.36). In line with prior recommendations (Ji et al., 2022), noise components were manually labeled based on both spatial and temporal features. In the spatial domain, components showing banding patterns, ring-like patterns at the edge of the brain, or with clusters primarily located in the white matter or cerebrospinal fluid were labeled as noise. In temporal and frequency domains, components with high-frequency peaks or sudden jumps in signal magnitude (caused by segment concatenation) were labeled as noise. Noise components were removed using the "fsl_regfilt" function. This approach resulted in 60% of components being labeled as noise, on average, across fetuses. Visual inspection of images suggests that this denoising approach led to reduction in spatial banding patterns, intensity inhomogeneity, and abnormal signal oscillations caused by rapid motion or segment concatenation.

2.3 | Quantification of fetal motor behavior

In parallel to the manual masking procedures described above, a process was performed to quantify fetal movement across all acquired fMRI scan data. Raw fMRI volumes were auto-masked by the CNN model developed by Rutherford et al. (2021). Twenty-two subjects (GA, mean = 34.50, *SD* = 2.72 weeks) were excluded due to the brain detection failure by the CNN, which related to poor image quality or large displacements of the brain from the image origin, resulting in a final sample of $n = 98$. After fetal brain extraction, the FSL MCFLIRT realignment tool (Jenkinson et al., 2002) was used to estimate a linear

transformation between a volume n to the middle volume as the reference. This step creates a text file that summarizes the six rigid-body realignment parameters across time. Frame-wise displacements (FDs) were then calculated as the sum of the absolute temporal derivatives of the six motion parameters between a volume n to the next volume $n+1$. Rotational parameters were transformed to millimeters by computing the arc length displacement on the surface of a sphere with radius of 30 mm, according to the following equation:

$$FD(t) = \sum |d(t-1) - d(t)| + 30 \times (\pi/180) \times \sum |r(t-1) - r(t)|$$

where $d(t)$ denotes translational motion parameters of tth volume, and the $r(t)$ is rotational parameters. The radius of 30 mm accounts for the smaller size of the fetal brain and scales with the standard used for adult MR image analysis (50 mm; Power et al., 2012).

We used the average FD, maximum FD, and maximum displacement relative to reference to quantify the motor behavior of the fetus during a scan. The average FD and maximum FD measure the brain location changes in every 2 s, while the maximum displacement measures the maximum movement over the entire 12 min. The motor behavior captured by fMRI of a representative subject (GA = 32) is shown in Figure 1. Henceforth, we use "Motor behavior" to refer to fetal behavior as measured by average FD, maximum FD, and the maximum displacement across a full ~12-min period. In contrast, "head motion" will refer to contaminant motion that remains within the analyzed neural network data (described below in Section 2.4), extracted from 100 low-motion volumes. In this way, head motion serves as measurement of a potential confound, whereas motor behavior references how much activity occurred in that fetus during the full EPI run. It was necessary to hold the number of volumes consistent across subjects, as varied data quantity may cause differential subject contribution to the k-means cost function, and because varied-length data in CAP analyses have yet to be validated. Finally, to ensure the quality of the movement estimation and registration, we evaluated the accuracy of alignment after FSL MCFLIRT motion correction. Specifically, in a subsample of 10 subjects, we employed Dice coefficient (Dice, 1945) to quantify volume overlap between each volume to the reference (the middle volume), following priors (Liao et al., 2019). The workflow of the full analysis is shown in Figure 2.

2.4 | Whole-brain CAP analysis with seeds in bilateral SMAs

We analyzed fetal supplementary motor CAPs, which are thought to reflect alternating brain states. Patterns expressed in each volume (all participants over time) are evaluated and clustering is used to isolate patterns that are repeated. More specifically, the process employs k-means clustering which allocates each data point to the nearest cluster, while reducing the within-cluster sum of squares. In this way, patterns that re-occur overtime are represented as CAPs, and CAPs are distinct from one another. The method does not depend on correlation in signal over the time series; instead, voxels contained within an individual CAP return to the same level of activity when that CAP

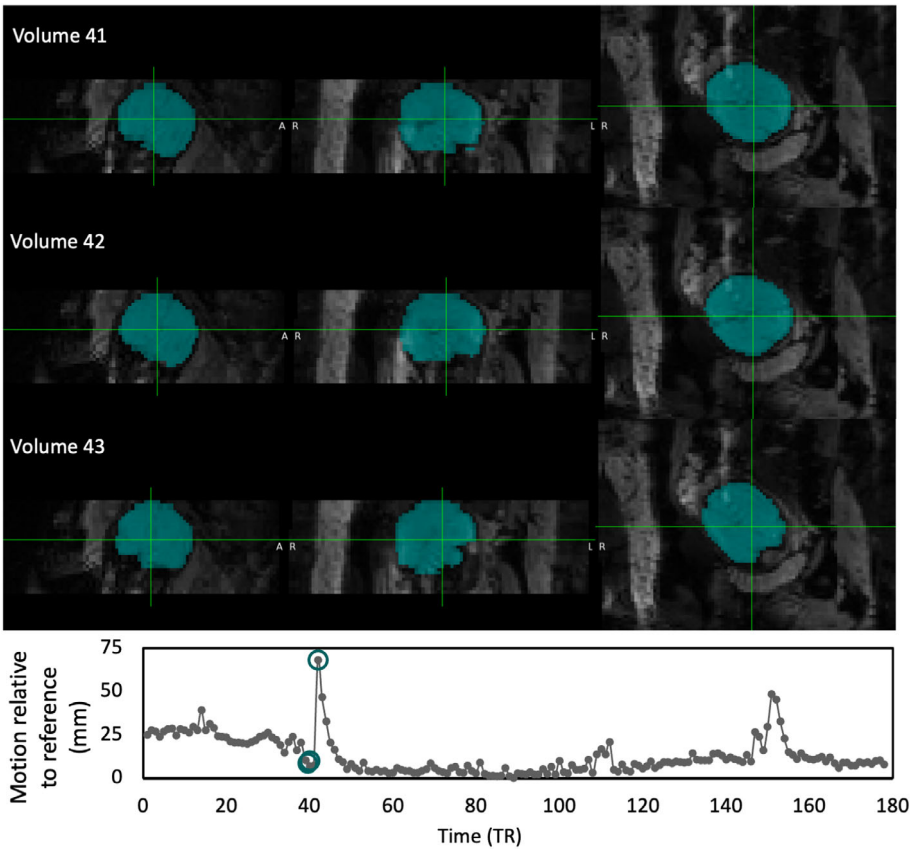

FIGURE 1 An example (GA = 32 weeks) of fetal motor behavior captured by fMRI. Top panels depict three fetal brain volumes drawn from a period of extreme repositioning. The mask used to segment the volume at each time is shown in turquoise. The brains approximate coronal, sagittal, and axial views, left to right. Plotted, below, is the frame-wise displacement (FD) over the time series. Circles in the lower plot indicate the time point corresponding to the brain figures shown in top panels. fMRI, functional magnetic resonance imaging; GA, gestational age.

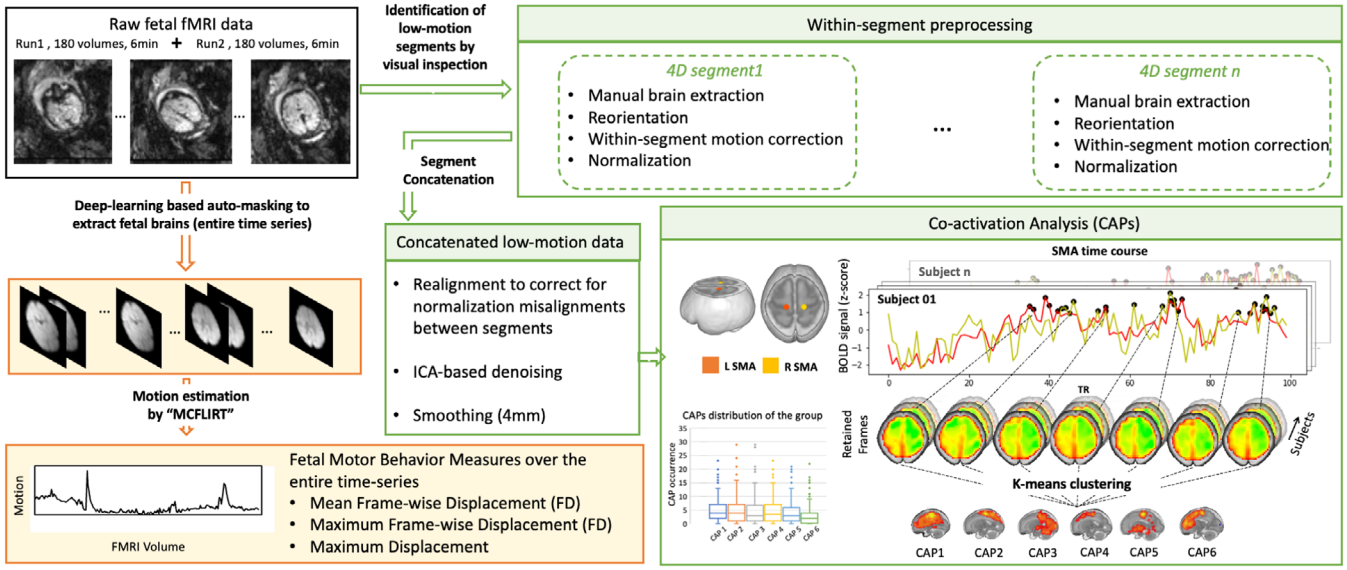

FIGURE 2 Workflow of the full analysis. For each subject, a 12-min scan, or two 6-min fMRI scans, was auto-masked by the deep learning model. The "MCFLIRT" realignment tool was then applied to the resulting 4D extracted brain series, to generate motion parameters for the full-time series. Fetal motor behavior measures of mean frame-wise displacement (FD), max FD, and maximum displacement were derived from the output of this realignment step. FD measures reflect the magnitude of brain location changes from volume to volume, while the maximum displacement measures the maximum movement over the entire 12 min. All the above steps are framed within yellow boxes. In parallel, the CAPs analysis was conducted only on the low-motion data (indicated by light green boxes). fMRI volumes with significant head motion were manually identified, using FSL image viewer, and excluded. Remaining segments of relatively low-motion fMRI data are henceforth referred to as "the low-motion segments." For each 4D low-motion segment, manual masking, reorientation, motion correction, and normalization to a 32-week fetal brain template (Serag et al., 2012) were performed. Preprocessed segments were then concatenated to form a single series and realignment was applied to correct potential misalignment between segments. This was followed by ICA-denoising and smoothing. CAP analysis was conducted on the first 100 processed volumes, which assures consistent quantity of data across subjects. CAP, coactivation pattern; fMRI, functional magnetic resonance imaging; ICA, Independent Component Analysis.

occurs. A further distinction in this method is that this k-means clustering is applied only to time points that are selected a priori. Specifically, individual time series are extracted from ROIs or voxels of interest, and peaks of activity for those regions define what will be considered in the k-means clustering. This additional step enables isolations of CAPs relevant to areas of focal interest.

CAP analyses utilized the tbCAPS toolbox (Bolton et al., 2020) to implement these steps: (1) FMRI volumes with supra-threshold signal ($z > 1$) in seed regions of each subject were selected as a feature set for following steps. Seeds were placed in the bilateral supplementary motor areas (SMAs); (2) classification of extracted volumes from all subjects into 6 clusters based on their spatial similarity using k-means clustering; and (3) averaging fMRI volumes assigned to same cluster to generate CAP maps. In the present study, Step 1 of the CAP method yielded 3230 time points. Robustness of clustering was assessed across candidates from $K = 2$ to $K = 8$ using a subsample of 90% of data, similar to priors (Monti et al., 2003). Stability and the CAP maps for different cluster numbers K are provided in Figure S1. Occurrences for each CAP were computed to describe the spatiotemporal features, which correspond to the total number of volumes assigned to each CAP for each subject. Given that the concatenation of low-motion periods introduces larger jumps in time-series data and interrupts the continuousness, transitions between CAPs were not examined in this study. In addition, a CAP analysis including all usable low-motion data is provided for comparison, in Figure S2.

We selected bilateral SMA seeds based on previous studies of our group (Thomason et al., 2015) with primary interest in isolating motor network hubs. Seeds were constructed using Mango Multi-image Analysis software (http://ric.uthscsa.edu/mango/mango.html). They were defined manually as spheres with a 3 mm radius (179 voxels), centered on MNI coordinates at (−9.5, −5.2, 22.3) and (9.5, −5.2, 22.3), with approximate locations of the bilateral SMA on a 32-week fetal template (Serag et al., 2012). The seed masks are available online at https://www.brainnexus.com/.

To ensure that CAPs were not contaminated by motion artifacts, we conducted correlation analyses of the CAP occurrence and duration with motion parameters derived from the realignment of images used in CAPs analysis.

2.5 | Assessment of postnatal motor behavior

At 7- and 36-month postpartum, infants' developmental skills were assessed with the Bayley Scales of Infant Development (3rd ed.; Bayley-III; Bayley; Bayley, 2006). In the current study, fine and gross motor subtests, as well as a scaled composite motor score, were evaluated. Given high correlations among Bayley motor subtests (see

Figure S3), the scaled composite motor score was used for longitudinal analyses. The motor composite ranges from 45 to 145. Scores ranging from 85 to 115 are considered typical motor development, while scores at or below 70 are indicative of a developmental delay at 2 standard deviations below the mean. Our sample showed a mean Bayley composite score of 96.90 ($SD = 14.23$, $n = 77$) at 7 months, and 98.49 ($SD = 11.58$, $n = 89$) at 36 months.

2.6 | Statistical analysis

All Statistical analyses were performed using SPSS (version 25). Relationships among motor behavior, age, and CAP occurrence were first examined using pairwise Pearson correlation analysis. Additional correlation analyses between motor behavior, age, and CAP occurrence were stratified by fetal sex. We then conducted six linear regression analyses to predict fetal motor behavior based upon age, sex, and occurrence of the six CAPs, respectively. CAP occurrences and maximum head displacement were log-transformed due to high skewness to ensure there was no violation of the assumption of normality and linearity. We further tested the predictive effect of fetal motor behavior and fetal CAPs on postnatal outcomes using a partial correlation that controlled for GA of scan and fetal sex. Cook's distances were estimated for regression models to assess potential outliers (values > 1). Results were deemed significant if they pass a threshold of $p < .008$ (.05/6 CAPs) as a Bonferroni adjustment for multiple comparison correction.

TABLE 2 Quality control on the fMRI data set

	Entire fMRI scans in evaluation of behavior ($n = 98$)	Low-motion fMRI periods that included in CAPs analysis ($n = 120$)
	Mean (SD)	Mean (SD)
Number of fMRI volumes	361.83 (79.64)	165.00 (52.72)
Observed fetal motion		
Mean translation (mm)	2.17 (1.31)	0.23 (0.10)
Max translation (mm)	11.82 (7.51)	0.87 (0.30)
Mean rotation (°)	0.11 (0.08)	0.39 (0.18)
Max rotation (°)	0.74 (0.53)	1.23 (0.43)

Abbreviations: CAP, coactivation pattern; FD, frame-wise displacement; fMRI, functional magnetic resonance imaging; SD, standard deviation.

3 | RESULTS

3.1 | Variation in fetal motor behavior with advancing GA

Fetal motor behavior was assessed in 98 fetuses (mean GA = 32.44, $SD = 3.90$ weeks) in which the CNN performance demonstrated high reliability. Detailed study sample demographic characteristics are provided in Table 1. The group average mean FD was 4.78 mm ($SD = 2.24$ mm), max FD was 44.72 mm ($SD = 32.50$ mm), and maximum brain displacement was 40.02 mm ($SD = 34.08$ mm). Raw motion measures are provided in Table 2, including both motion measured across the entire scan (estimate for motor behavior) and motion measured in low-motion periods of fMRI data that were included in neuroimaging analyses.

GA was negatively correlated with all above three motor behavior measures across the entire scan, with $r = -.51$ ($p < .001$) for mean FD, $r = -.37$ ($p < .001$) for max FD, and $r = -.25$ ($p = .01$) for the max displacement over the entire scan, respectively (Figure 3). For the majority of subjects ($n = 88$), 360 volumes (12 min, TR = 2 s fMRI scan) were used in motor behavior measurement. A small number of cases had 180 ($n = 6$), 540 ($n = 1$), or 720 ($n = 3$) volumes due to interrupted or additional repeat scans. Sensitivity analysis on the subset of 88 cases with 360 volumes, confirmed that the significant relationship between motor behavior and age remained (mean FD: $r = -.50$, $p < .001$, max FD: $r = -.37$, $p < .001$, max displacement: $r = -.27$, $p = .01$). Correlation analyses between fetal motor behavior

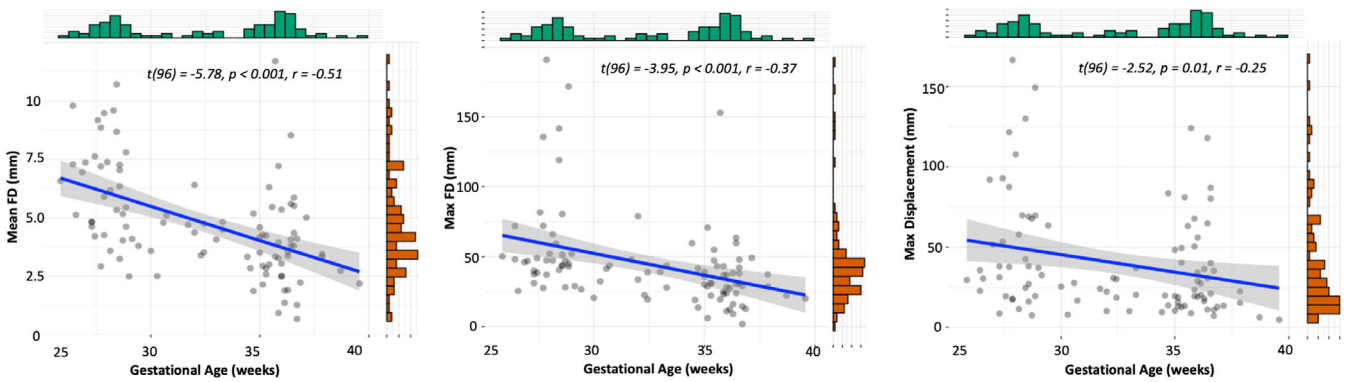

FIGURE 3 Motor behavior changes across gestational age. Fetal mean (left) and max (middle) frame-wise displacement (FD), and the maximum brain displacement (right) across all volumes in the fMRI scan are all negatively correlated with gestational age. fMRI, functional magnetic resonance imaging.

and GA by sex group are provided in Figure S4. In addition, the secondary analysis evaluating performance of movement estimation suggested that images were well aligned after motion correction. Indeed, volume overlap with the reference image was 88% on average (Figure S5).

3.2 | Observed SMA CAPs

About 3230 fMRI volumes (26.9% of the total time) showing suprathreshold high signal in either left or right SMA regions were included in the subsequent k-means clustering. Brain regions coactivated with bilateral SMA were clustered into six stable spatial patterns (CAP maps) as shown in Figure 4. The first CAP, which included 19% of the total included fMRI volumes from all subjects, overlapped within the right parietal regions. The second CAP (18% of the total) reflected coactivation localized in the bilateral SMA. The third CAP (18% of the total) involved the posterior part of the right hemisphere, extending to occipital regions. The fourth CAP (18% of the total) was similar to the second CAP showing bilateral SMA coactivation, but was more left lateralized. The fifth CAP (15% of the total) was considered a left parietotemporal network, mostly within the motor network but including subcortical regions. The sixth CAP (12% of the total) constituted right frontal regions. A figure presenting equal distribution of CAPs across subjects is provided in Figure S6, suggesting that the clustering was not driven by individual-level variance.

Pearson correlation analyses between CAP occurrence and age revealed one primary effect. We observed that CAP1 occurrence was marginally negatively correlated with GA ($r = -.19$, $p = .06$, Figure 4). That is, with advancing age, presence of CAP 1 was reduced. Correlation between CAP occurrence and GA by sex is provided in Figure S7.

3.3 | Linear regression models of fetal motor behavior and CAP features

Linear regression revealed significant linkage between fetal motor behavior across the entire scan and CAP5 occurrence during low-motion segments (F (3, 94)= 6.57, $p < .001$, $R^2 = .173$), controlling for age and sex. In this model, age ($\beta_{(age)} = -.27$, $p = .005$) and CAP5 occurrence ($\beta_{(CAP5)} = -.29$, $p = .003$) were both statistically significant. Occurrences of other CAPs did not show a significant

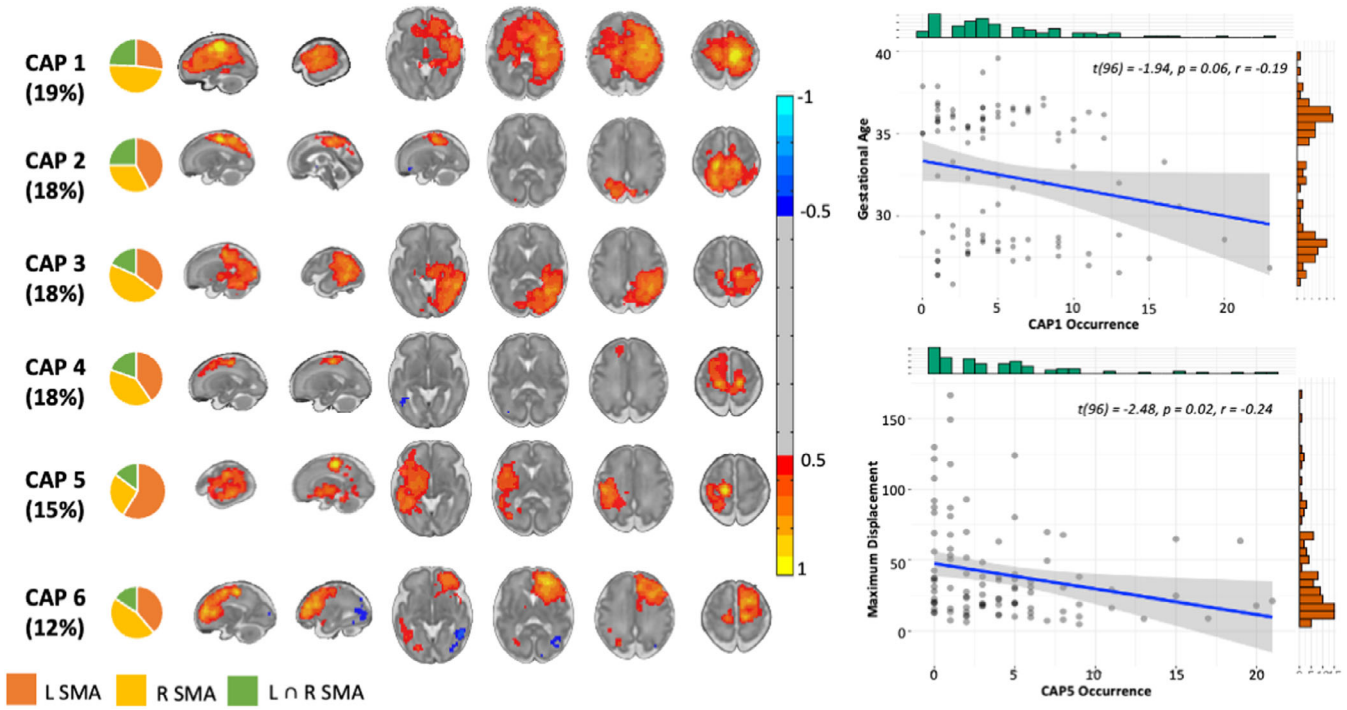

FIGURE 4 SMA-CAPs. The six SMA CAPs (z values, thresholded at $|z| > 0.5$) are displayed on the left, with pie charts indicating the amount of time each pattern coactivated with the left SMA, right SMA, or bilateral SMA seeds. CAPS were calculated on the first 100 low-motion fMRI volumes. More frequent CAP 1 occurrence was marginally correlated with lower fetal gestational age (top right) and more frequent CAP 5 occurrence was significantly correlated with lower fetal maximum brain displacement across the entire fMRI scan. The frequency of CAP1 and CAP5 occurrence is indicated on the top X axis of both scatterplots and the frequency of GA and max FD values is indicated on the right Y axis of each plot, respectively. There were no other significant associations between CAP occurrence, fetal gestational age, and fetal motor behavior. CAP, coactivation pattern; FD, frame-wise displacement; fMRI, functional magnetic resonance imaging; GA, gestational age; SMA, supplementary motor area.

TABLE 3 Summary of regression models predicting fetal motor behavior upon age, sex, and the occurrences

	R^2	*F (3, 94)*	*F. sig (p value)*	CAP *T. sig (p value)*
Model 1: Max FD ~ Age + sex + CAP1 occurrence	0.097	3.351	.022	.453
Model 2: Max FD ~ Age + sex + CAP2 occurrence	0.092	3.192	.027	.712
Model 3: Max FD ~ Age + sex + CAP3 occurrence	0.095	3.297	.024	.518
Model 4: Max FD ~ Age + sex + CAP4 occurrence	0.093	3.211	.027	.665
Model 5: Max FD ~ Age + sex + CAP5 occurrence	0.173	6.571	<.001*	.003*
Model 6: Max FD ~ Age + sex + CAP6 occurrence	0.091	3.143	.107	.954

*Significant regression model with $p < 0.008$.

association with fetal motor behavior (Table 3). Thus, occurrence of coactivation of the left parietal–temporal network was isolated as the single CAP associated with fetal motor behavior.

We did not find evidence to suggest that expression of CAP5 was related to motion artifacts in low-motion images used in fMRI analysis. That is, CAP5 occurrence was not related to any weighted averaged head motion parameters derived from the realignment of usable, low-motion data segments (mean translational displacements: $r = -.07$, $p = .47$; maximum translation displacements: $r = -.05$, $p = .59$; mean rotation: $r = -.03$, $p = .76$; maximum rotation: $r = -.06$, $p = .53$). It is important to realize that this analysis showed that the occurrence of CAP5 was related to fetal motor behavior across the whole of the rest of the scan, not to motion within the fMRI segment analyzed.

The additional CAP analysis including all usable data showed similar CAP maps, but CAP occurrence no longer showed a significant correlation with motor behavior. We expect the latter finding results from normalization of values by fMRI volume count, as the volume count was related to motor behavior.

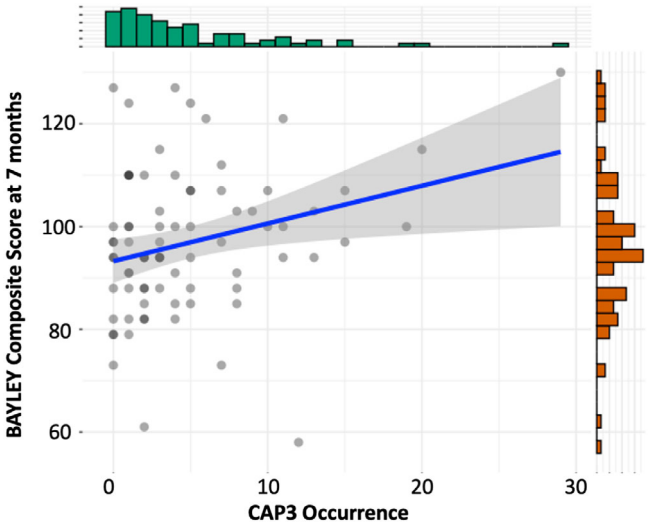

FIGURE 5 Prediction effect of CAP3 occurrence on postnatal motor function (Bayley Composite score) at 7 months. Fetuses who spent more time in CAP 3, representing coactivation of right occipital regions with the SMA seeds, had more mature motor abilities at 7 months after birth. The distribution of Bayley motor composite scores is displayed on the right Y axis and the distribution of CAP 3 occurrence is displayed on the top X axis. CAP, coactivation pattern; SMA, supplementary motor area.

3.4 | Prediction effect of CAP features to postnatal motor behavior

We did not find significant correlation between fetal motor behavior and any postnatal motor outcomes. However, CAP3 occurrence was prospectively associated with 7-month Bayley composite score ($r = .43$, $p = .03$, Figure 5), controlling for GA at scan and sex. We observed a positive association suggesting that more time spent in CAP3, comprised of right parietal-posterior regions, during fetal resting-state was prospective associated with improved motor outcome at age 7 months.

4 | DISCUSSION

In this study, we applied a novel, automated fMRI-based approach for analyzing fetal motor behavior. Compared to methods that manually assess motor behavior (De Vries & Fong, 2007; Hayat et al., 2011), automated approaches are less subject to potential bias, or subjectivity, and are less labor intensive. We discovered that natural movements of fetuses during fMRI scans, which have long been considered barriers to effective imaging, can be quantified as meaningful indicators of fetal behavior. This fMRI-based behavioral movement approach confirms the decreasing occurrence of motor activity with increasing GA, observed previously with other imaging modalities such as ultrasound (Ten Hof et al., 2002) and cine MRI (Hayat et al., 2011). In addition, we examined the fetal neural motor network (SMA) using CAP analysis, a methodology that defines multiple CAPs, or "states," for a given region and then classifies time spent in each state. Results suggested the intrinsic CAPs of SMA shifts between hemispheres, and between anterior and posterior brain regions over time. Specifically, less time spent in a brain state localized in motor network regions (CAP1 and CAP5) was correlated with increased GA or increased motor behavior. More time spent in a state linking SMA to posterior brain regions related to

future infant motor behavior at 7 months. Extending previous observations of fetal "static" networks, our results demonstrate that the occurrence of a fetal motor subnetwork is associated with fetal behavior and postnatal motor outcomes. Concurrent measurement of fetal behavior and fetal brain activity presents a new interface at which to evaluate cognitive developmental and clinical neuroscience research questions.

Our results replicate prior work showing decreased "general movements" of the fetus across gestation (Hayat et al., 2011; Ten Hof et al., 2002). In utero spatial constraint secondary to fetal growth is likely one factor that drives the observed decrease in gross fetal movement across gestation. Consistent with this interpretation, rat fetuses raised in a bath completely removed from all membranes show higher activity levels by embryonic Day 21 compared to fetuses growing in utero or in amnion (i.e., externalized from the maternal compartment, but within amniotic membranes; Ronca et al., 1994). In addition to spatial constraints, lower movement levels may be favored later in gestation, a time when the larger fetal body places greater demands on oxygen delivery from the placenta. Reduced fetal head movement could also reflect maturing behavior patterns following the emergence of inhibitory cortical influences as the corpus callosum develops (Malinger & Zakut, 1993). As general movements decrease, goal-directed isolated movements have been shown to increase across gestation (Fagard et al., 2018). Indeed, the most frequent fetal movements in the third trimester serve functional purposes in the postnatal world, such as hand to face, scowling, eye opening, and mouthing (Kurjak et al., 2004). The fMRI-based method for quantifying fetal motor behavior implemented in the present study does not allow for detection of these fine-grained movements, and instead likely reflects gross motions of body and head. The onset of fetal sleep, which begins at ~28-week postconception (Peirano et al., 2003), may also contribute to decreased fetal movements as sleep states tend to cause less frequent and smaller motion (Hayat et al., 2011).

The present study investigated fetal motor system dynamics using the method of CAPs analysis, which enables evaluation of a given network, as a collection of subsystems that move in and out of synchrony. Compared to the sliding-window approach and other multivariate approaches, such as independent component analysis, CAPs analysis provides observations of state alternations with the temporal resolution of individual fMRI volumes. In contrast to "static" functional connectivity analysis that has revealed a single connectivity pattern of the SMA in fetal brains (Thomason et al., 2018), our dynamic approach indicated that the fetal SMA alternates between six distinct CAPs. We observed negative correlations between occurrence of within-motor network patterns (CAP1 and CAP5) with age and motor behavior, respectively, which may reflect a maturational pattern in which the motor network is connecting to increasingly distant regions outside of canonical motor regions with advancing GA. This is in line with prior observations from graph theoretical analyses, showing that modularity decreases and efficiency increases with advancing GA (Thomason et al., 2014; Turk et al., 2019). Steps taken toward development of an integrated network before birth may prime the brain for continued development of long-range connections in the postnatal period. In the postnatal period, these long-range connections will be refined through pruning processes, giving rise to segregation between, and integration within, specialized brain networks, a pattern typical of the more mature human brain (Zhao et al., 2019).

We also found that increased occurrence of CAP3, reflecting coactivation between SMA and posterior brain regions, including the visual cortex, was prospectively related to the infant motor development. The establishment of connectivity between motor and visual cortex may represent the global shift from more local to long-range connectivity, described above, or it may reflect priming of coordination between motor and visual systems. Further, increased coupling between these systems may provide a potential scaffolding mechanism for the phenomena of future motor learning by observing (McGregor & Gribble, 2015). In contrast, the connection between motor and prefrontal regions (CAP 6) showed no predictive effect, which fits with the slower maturational timeline of the prefrontal cortex (Hodel, 2018). It should be noted that the present study did not find a significant association between prenatal motor activity and postnatal motor outcomes. A prior examination by Hayat et al. (2018), linking prenatal cine MRI motion measures with Bayley outcomes, found that fetal motor behavior predicted outcome only in a risk group, not in a neurotypical sample, suggesting there may be important individual differences to be considered in comparison of pre- and postnatal motor measurements.

The naturally occurring CAPs observed for the fetal SMA included three components that were both lateralized and related to behavioral variation (CAP1, CAP3, and CAP5). Further study of inter- versus intra-hemispheric networks that develop over human gestation warrant further study. Hemispheric asymmetries are observed for a variety of structures beginning in the second trimester (Machado-Rivas et al., 2022; Vasung et al., 2020), including greater leftward asymmetry for temporal structures early in development (Kasprian et al., 2011; Vasung et al., 2020). In adulthood, functional lateralization has been observed for symbolic communication, emotion, decision-making, and of particular relevance for the present study, sensory perception and action (Karolis et al., 2019). This lateralization is hypothesized to minimize inefficient conduction across hemispheres and optimize faster informational exchanges between relevant neuronal groups. Given this is the first application of the CAP methodology in fetal fMRI data, there is considerable opportunity for future work examining other sensory modalities with further evaluation of hemispheric versus global patterns in relative occurrence of CAPs.

Detailed characterization of the function and cause of fetal movements is an important area for future investigation. Here, general motion was evaluated and physiological and sleep states were not assessed. Further, the genesis of movement in this context is not known. That is, fetal movement can result from extrinsic experiences, such as movement of the mother and sequence-related variation in sound and temperature (Gowland & De Wilde, 2008). There is opportunity to build on the deep learning approach applied here, for example, by adding measures of fetal eye movements or physiology that relay information about naturally occurring fetal sleep states. Other studies might address the behavioral response of the fetus to the

presentation of stimuli. Pioneering fetal task-based fMRI studies have been achieved, but these have been conducted in very small sample sizes and fetal behavior was not quantified (see review by Anderson & Thomason, 2013).

Notable work by Schöpf et al. (2014) has demonstrated a link between in-utero spontaneous fetal eye movements to simultaneous resting-state activation in visual, motor, and orbitofrontal areas in seven fetuses. In this study, eye center locations were tracked over time computationally with the aid of a machine learning-based eye detection algorithm in fMRI data. The opportunity to leverage simultaneously collected biological and behavioral measurements is an important direction for future research on fetal development.

Another consideration for the current study is application of FSL MCFLIRT for motion estimation. There is potential that emerging novel registration algorithms may be better for addressing motion in fetal functional MRI data (Liao et al., 2019; Scheinost et al., 2018; Sobotka et al., 2022). Even though our deep learning approach has provided us with precise masks, the lack of detailed structure in fetal fMRI contrast with the rather coarse resolution ($3.4 \times 3.4 \times 4$ mm^3), can still hinder optimal registration. As the field of fetal fMRI advances, it may serve well to explore alternate methods for motion estimation, with potential for improved sensitivity.

It is useful to also consider potential for sample selection bias in the present study. Given the high criteria of the image quality required by the brain activity analysis, we had to exclude many fMRI volumes, and in some cases, had to exclude subjects, both with potential to introduce bias. We hope future studies could improve upon this situation by including more fMRI volumes with advanced image reconstruction approaches. With more data, it may also be possible to analyze fetal brain activity before initiation of a movement; one could begin to examine order effects, and could possibly link neural patterns to specific behavioral functions. Another consideration regarding the current study is that the Bayley scale we used here is designed to assess general infant development, rather than to specifically assess motor outcomes. In future studies, more targeted assessments of motor development, such as the Alberta Infant Motor scale (Piper et al., 1992), may provide new knowledge in relation to our fetal motor and brain measures. A final point to consider is that analyses undertaken in the current study do not include sensitivity or specificity analyses, which would be useful for estimating robustness of SMA CAPS as a predictor of infant behavior. Future work using machine learning and other complementary approaches will further strengthen the understanding of the predictive value of these brain–behavior associations at the individual level.

The present study identified unique network dynamics that covaried with pre- and postnatal motor behavior using a novel deep learning methodology. Findings suggest that time spent in a state comprised of common activation patterns across motor regions was inversely related to age and amount of motor activity during the scan, supporting the idea that global integration (rather than segregation) increases with fetal maturation. The present study also provided the first characterization of substate organization of a given brain network, here, the motor network. Utilization of the CAP technique is valuable for moving beyond static, fixed representations of connectivity across brain systems of interest. The methods introduced in this study provide a new and promising tool for investigating fetal brain maturation. There is opportunity for methods such as this to advance understanding of the ontology of developmental disorders and human neurological disease, as well as to better define trajectories of typical neural development.

ACKNOWLEDGMENTS

This project was supported by awards from the National Institutes of Health, MH110793, DA050287, MH122447, and ES032294. The authors thank Jasmine Hect and Pavan Jella for their assistance in data acquisition and acknowledge Saige Rutherford as contributing to the techniques used in this study. Importantly, the authors thank participant families who generously shared their time and expressed interest in helping future babies and children to achieve their best possible health outcomes.

CONFLICT OF INTEREST

The authors declare no conflict of interest.

DATA AVAILABILITY STATEMENT

The data and code used in this study will be made available via https://ndar.nih.gov/ and/or accessed upon direct request to M.E. Thomason (data) or L. Ji (code).

ORCID

Lanxin Ji https://orcid.org/0000-0003-4509-0225

REFERENCES

Anderson, A. L., & Thomason, M. E. (2013). Functional plasticity before the cradle: A review of neural functional imaging in the human fetus. *Neuroscience & Biobehavioral Reviews*, *37*(9), 2220–2232.

Bayley, N. (2006). *Bayley scales of infant and toddler development*. PsychCorp, Pearson.

Blazejewska, A. I., Seshamani, S., McKown, S. K., Caucutt, J. S., Dighe, M., Gatenby, C., & Studholme, C. (2017). 3D in utero quantification of T2* relaxation times in human fetal brain tissues for age optimized structural and functional MRI. *Magnetic Resonance in Medicine*, *78*(3), 909–916. https://doi.org/10.1002/mrm.26471

Bolton, T. A., Tuleasca, C., Wotruba, D., Rey, G., Dhanis, H., Gauthier, B., Delavari, F., Morgenroth, E., Gaviria, J., Blondiaux, E., Smigielski, L., & Van De Ville, D. (2020). TbCAPs: A toolbox for co-activation pattern analysis. *NeuroImage*, *211*, 116621.

De Vries, J., & Fong, B. (2007). Changes in fetal motility as a result of congenital disorders: An overview. *Ultrasound in Obstetrics and Gynecology: The Official Journal of the International Society of Ultrasound in Obstetrics and Gynecology*, *29*(5), 590–599.

Dice, L. R. (1945). Measures of the amount of ecologic association between species. *Ecology*, *26*(3), 297–302.

DiPietro, J. A., Kivlighan, K. T., Costigan, K. A., Rubin, S. E., Shiffler, D. E., Henderson, J. L., & Pillion, J. P. (2010). Prenatal antecedents of newborn neurological maturation. *Child Development*, *81*(1), 115–130.

Dipietro, J. A., Voegtline, K. M., Pater, H. A., & Costigan, K. A. (2018). Predicting child temperament and behavior from the fetus. *Development and Psychopathology*, *30*(3), 855–870.

Dutton, P. J., Warrander, L. K., Roberts, S. A., Bernatavicius, G., Byrd, L. M., Gaze, D., Kroll, J., Jones, R. L., Sibley, C. P., Frøen, J. F., & Heazell, A. E.

(2012). Predictors of poor perinatal outcome following maternal perception of reduced fetal movements–a prospective cohort study. *PLoS One*, *7*(7), e39784.

Fagard, J., Esseily, R., Jacquey, L., O'regan, K., & Somogyi, E. (2018). Fetal origin of sensorimotor behavior. *Frontiers in Neurorobotics*, *12*, 23.

Gowland, P., & De Wilde, J. (2008). Temperature increase in the fetus due to radio frequency exposure during magnetic resonance scanning. *Physics in Medicine & Biology*, *53*(21), L15–L18.

Guzzetta, A., Mercuri, E., Rapisardi, G., Ferrari, F., Roversi, M., Cowan, F., Rutherford, M., Paolicelli, P. B., Einspieler, C., Boldrini, A., Dubowitz, L., Prechtl, H. F., & Cioni, G. (2003). General movements detect early signs of hemiplegia in term infants with neonatal cerebral infarction. *Neuropediatrics*, *34*(2), 61–66.

Hayat, T., Martinez-Biarge, M., Kyriakopoulou, V., Hajnal, J. V., & Rutherford, M. A. (2018). Neurodevelopmental correlates of fetal motor behavior assessed using cine MR imaging. *American Journal of Neuroradiology*, *39*(8), 1519–1522.

Hayat, T., Nihat, A., Martinez-Biarge, M., McGuinness, A., Allsop, J., Hajnal, J., & Rutherford, M. (2011). Optimization and initial experience of a multisection balanced steady-state free precession cine sequence for the assessment of fetal behavior in utero. *American Journal of Neuroradiology*, *32*(2), 331–338.

Hayat, T., & Rutherford, M. (2018). Neuroimaging perspectives on fetal motor behavior. *Neuroscience & Biobehavioral Reviews*, *92*, 390–401.

Hielkema, T., & Hadders-Algra, M. (2016). Motor and cognitive outcome after specific early lesions of the brain—A systematic review. *Developmental Medicine & Child Neurology*, *58*, 46–52.

Hodel, A. S. (2018). Rapid infant prefrontal cortex development and sensitivity to early environmental experience. *Developmental Review*, *48*, 113–144.

Jakab, A., Schwartz, E., Kasprian, G., Gruber, G. M., Prayer, D., Schöpf, V., & Langs, G. (2014). Fetal functional imaging portrays heterogeneous development of emerging human brain networks. *Frontiers in Human Neuroscience*, *8*, 852. https://doi.org/10.3389/fnhum.2014.00852

Jenkinson, M., Bannister, P., Brady, M., & Smith, S. (2002). Improved optimization for the robust and accurate linear registration and motion correction of brain images. *NeuroImage*, *17*(2), 825–841.

Ji, L., Hendrix, C. L., & Thomason, M. E. (2022). Empirical evaluation of human fetal fMRI preprocessing steps. *Network Neuroscience*, *6*(3), 702–721. https://doi.org/10.1162/netn_a_00254

Karolis, V. R., Corbetta, M., & Thiebaut de Schotten, M. (2019). The architecture of functional lateralisation and its relationship to callosal connectivity in the human brain. *Nature Communications*, *10*(1), 1–9.

Kasprian, G., Langs, G., Brugger, P. C., Bittner, M., Weber, M., Arantes, M., & Prayer, D. (2011). The prenatal origin of hemispheric asymmetry: An in utero neuroimaging study. *Cerebral Cortex*, *21*(5), 1076–1083.

Kurjak, A., Stanojevic, M., Andonotopo, W., Salihagic-Kadic, A., Carrera, J. M., & Azumendi, G. (2004). Behavioral pattern continuity from prenatal to postnatal life a study by four-dimensional (4D) ultrasonography. *Journal of Perinatal Medicine*, *32*(4), 346–353.

Liao, R., Turk, E. A., Zhang, M., Luo, J., Adalsteinsson, E., Grant, P. E., & Golland, P. (2019). Temporal registration in application to in-utero MRI time series. arXiv preprint arXiv:1903.02959.

Liu, X., Chang, C., & Duyn, J. H. (2013). Decomposition of spontaneous brain activity into distinct fMRI co-activation patterns. *Frontiers in Systems Neuroscience*, *7*, 101.

Liu, X., Zhang, N., Chang, C., & Duyn, J. H. (2018). Co-activation patterns in resting-state fMRI signals. *NeuroImage*, *180*, 485–494.

Machado-Rivas, F., Gandhi, J., Choi, J. J., Velasco-Annis, C., Afacan, O., Warfield, S. K., Gholipour, A., & Jaimes, C. (2022). Normal growth, sexual dimorphism, and lateral asymmetries at fetal brain MRI. *Radiology*, *303*(1), 162–170.

Malinger, G., & Zakut, H. (1993). The corpus callosum: Normal fetal development as shown by transvaginal sonography. *American Journal of Roentgenology*, *161*(5), 1041–1043.

McGregor, H. R., & Gribble, P. L. (2015). Changes in visual and sensory-motor resting-state functional connectivity support motor learning by observing. *Journal of Neurophysiology*, *114*(1), 677–688.

Monti, S., Tamayo, P., Mesirov, J., & Golub, T. (2003). Consensus clustering: A resampling-based method for class discovery and visualization of gene expression microarray data. *Machine Learning*, *52*(1), 91–118.

Peirano, P., Algarín, C., & Uauy, R. (2003). Sleep-wake states and their regulatory mechanisms throughout early human development. *The Journal of Pediatrics*, *143*(4), 70–79.

Piper, M. C., Pinnell, L. E., Darrah, J., Maguire, T., & Byrne, P. J. (1992). Construction and validation of the Alberta infant motor scale (AIMS). *Canadian Journal of Public Health= Revue canadienne de sante publique*, *83*, 46–50.

Power, J. D., Barnes, K. A., Snyder, A. Z., Schlaggar, B. L., & Petersen, S. E. (2012). Spurious but systematic correlations in functional connectivity MRI networks arise from subject motion. *NeuroImage*, *59*(3), 2142–2154.

Prechtl, H. F. R., & Einspieler, C. (1997). Is neurological assessment of the fetus possible? *European Journal of Obstetrics & Gynecology and Reproductive Biology*, *75*(1), 81–84. https://doi.org/10.1016/S0301-2115(97)00197-8

Richards, T. W., & Newbery, H. (1938). Studies in fetal behavior: III. Can performance on test items at six months postnatally be predicted on the basis of fetal activity? *Child Development*, *9*(1), 79–86.

Ronca, A. E., Kamm, K., Thelen, E., & Alberts, J. R. (1994). Proximal control of fetal rat behavior. *Developmental Psychobiology: The Journal of the International Society for Developmental Psychobiology*, *27*(1), 23–38.

Rutherford, S., Sturmfels, P., Angstadt, M., Hect, J., Wiens, J., van den Heuvel, M. I., Scheinost, D., Sripada, C., & Thomason, M. (2021). Automated brain masking of fetal functional MRI with open data. *Neuroinformatics*, *20*(1), 173–185.

Scheinost, D., Onofrey, J. A., Kwon, S. H., Cross, S. N., Sze, G., Ment, L. R., & Papademetris, X. (2018). A fetal fMRI specific motion correction algorithm using 2nd order edge features. *Paper presented at the 2018 IEEE 15th international symposium on biomedical imaging (ISBI 2018)*.

Schöpf, V., Schlegl, T., Jakab, A., Kasprian, G., Woitek, R., Prayer, D., & Langs, G. (2014). The relationship between eye movement and vision develops before birth. *Frontiers in Human Neuroscience*, *8*, 775. https://doi.org/10.3389/fnhum.2014.00775

Serag, A., Aljabar, P., Ball, G., Counsell, S. J., Boardman, J. P., Rutherford, M. A., Edwards, A. D., Hajnal, J. V., & Rueckert, D. (2012). Construction of a consistent high-definition spatio-temporal atlas of the developing brain using adaptive kernel regression. *NeuroImage*, *59*(3), 2255–2265.

Shattuck, D. W., & Leahy, R. M. (2002). BrainSuite: An automated cortical surface identification tool. *Medical Image Analysis*, *6*(2), 129–142.

Sobotka, D., Ebner, M., Schwartz, E., Nenning, K.-H., Taymourtash, A., Vercauteren, T., Ourselin, S., Kasprian, G., Prayer, D., Langs, G., & Langs, G. (2022). Motion correction and volumetric reconstruction for fetal functional magnetic resonance imaging data. *NeuroImage*, *255*, 119213.

Ten Hof, J., Nijhuis, I. J., Mulder, E. J., Nijhuis, J. G., Narayan, H., Taylor, D. J., Westers, P., & Visser, G. H. (2002). Longitudinal study of fetal body movements: Nomograms, intrafetal consistency, and relationship with episodes of heart rate patterns a and B. *Pediatric Research*, *52*(4), 568–575.

Thomason, M. E. (2020). Development of brain networks in utero: Relevance for common neural disorders. *Biological Psychiatry*, *88*(1), 40–50.

Thomason, M. E., Brown, J. A., Dassanayake, M. T., Shastri, R., Marusak, H. A., Hernandez-Andrade, E., Yeo, L., Mody, S., Berman, S., Hassan, S. S., & Romero, R. (2014). Intrinsic functional brain architecture derived from graph theoretical analysis in the human fetus. *PLoS One*, *9*(5), e94423.

Thomason, M. E., Grove, L. E., Lozon, T. A., Jr., Vila, A. M., Ye, Y., Nye, M. J., Manning, J. H., Pappas, A., Hernandez-Andrade, E., Yeo, L., Mody, S., Berman, S., Hassan, S. S., & Romero, R. (2015). Age-related increases in long-range connectivity in fetal functional neural connectivity networks in utero. *Developmental Cognitive Neuroscience*, *11*, 96–104.

Thomason, M. E., Hect, J., Waller, R., Manning, J. H., Stacks, A. M., Beeghly, M., Boeve, J. L., Wong, K., van den Heuvel, M. I., Hernandez-Andrade, E., Hassan, S. S., & Romero, R. (2018). Prenatal neural origins of infant motor development: Associations between fetal brain and infant motor development. *Development and Psychopathology*, *30*(3), 763–772.

Turk, E., Van Den Heuvel, M. I., Benders, M. J., De Heus, R., Franx, A., Manning, J. H., Hect, J. L., Hernandez-Andrade, E., Hassan, S. S., Romero, R., Kahn, R. S., Thomason, M. E., & van den Heuvel, M. P. (2019). Functional connectome of the fetal brain. *Journal of Neuroscience*, *39*(49), 9716–9724.

van den Heuvel, M. I., Turk, E., Manning, J. H., Hect, J., Hernandez-Andrade, E., Hassan, S. S., Romero, R., van den Heuvel, M. P., & Thomason, M. E. (2018). Hubs in the human fetal brain network. *Developmental Cognitive Neuroscience*, *30*, 108–115. https://doi.org/10.1016/j.dcn.2018.02.001

Vasung, L., Rollins, C. K., Yun, H. J., Velasco-Annis, C., Zhang, J., Wagstyl, K., Evans, A., Warfield, S. K., Feldman, H. A., Grant, P. E., & Gholipour, A. (2020). Quantitative in vivo MRI assessment of structural asymmetries and sexual dimorphism of transient fetal compartments in the human brain. *Cerebral Cortex*, *30*(3), 1752–1767.

Zhao, T., Xu, Y., & He, Y. (2019). Graph theoretical modeling of baby brain networks. *NeuroImage*, *185*, 711–727.

SUPPORTING INFORMATION

Additional supporting information can be found online in the Supporting Information section at the end of this article.

How to cite this article: Ji, L., Majbri, A., Hendrix, C. L., & Thomason, M. E. (2023). Fetal behavior during MRI changes with age and relates to network dynamics. *Human Brain Mapping*, *44*(4), 1683–1694. https://doi.org/10.1002/hbm.26167